

# Base promoted decomposition of bis(1,4,7-triazacyclononane)nickel(III) in aqueous solution

Bernd Sonnberger, Peter Hühn, Andreas Waßerburger\* and F. Wasgestian\*\*

Institute of Inorganic Chemistry, University of Cologne, Greinstrasse 6, D-W 5000 Cologne 41 (Germany)

(Received November 18, 1991; revised March 9, 1992)

## Abstract

The base promoted decomposition of  $\text{NiL}_2^{3+}$  ( $L=1,4,7$ -triazacyclononane) in aqueous solutions was studied using UV-Vis spectroscopy and stopped-flow techniques. The overall stoichiometry was specified by product determinations. The reaction is initiated by deprotonation of  $\text{NiL}_2^{3+}$  producing  $\text{NiLL}_{\text{dp}}^{2+}$ . The absorption spectrum of the deep blue  $\text{NiLL}_{\text{dp}}^{2+}$  was recorded between 350 and 500 nm. The decomposition yields  $\text{Ni}_{\text{aq}}^{2+}$  and  $\text{NiL}(\text{H}_2\text{O})_3^{2+}$  (or their conjugate bases) in equal parts. It proceeds via mono- and bimolecular pathways. In the pH range 1–13.7 ( $I=0.1$  or  $1$  M ( $\text{NaClO}_4$ )) the following rate constants were obtained at  $24^\circ\text{C}$ : monomolecular decays of  $\text{NiL}_2^{3+}$  ( $k_{11}\approx 0$ ) and  $\text{NiLL}_{\text{dp}}^{2+}$  ( $k_{12}=0.5\pm 0.3\text{ s}^{-1}$ ) and the bimolecular rate constants of the reactions  $\text{NiL}_2^{3+} + \text{NiL}_2^{3+}$  ( $k_{21}=(6.0\pm 0.6)\times 10^{-5}\text{ M}^{-1}\text{ s}^{-1}$ ),  $\text{NiL}_2^{3+} + \text{NiLL}_{\text{dp}}^{2+}$  ( $k_{22}\approx 3\times 10^3\text{ M}^{-1}\text{ s}^{-1}$ ), and  $\text{NiLL}_{\text{dp}}^{2+} + \text{NiLL}_{\text{dp}}^{2+}$  ( $k_{23}=(7.3\pm 0.8)\times 10^4\text{ M}^{-1}\text{ s}^{-1}$ ).

## Introduction

Since the first observation [1] of a nickel(III) species in aqueous solution in 1972, considerable progress has been made to stabilize this oxidation state. In particular the use of polyaza cycloalkane ligands (macrocycles) has allowed the redox [2–14] and ligand substitution [15–17] behavior of Ni(III) in water to be studied. Aqueous solutions of nickel(III) amine complexes are generally stable under acid conditions [6]. The pH dependence of the decomposition rate was explained by the involvement of N-deprotonated species [18]. Kinetic studies have so far covered mainly coordinatively unsaturated tetraaza complexes [19–23] and pulse-radiolytically generated Ni(III) solutions [1, 24]. In both cases nickel(III) species participated in the reaction and gave rise to complicated overall rate laws. Moreover, no investigations over a wide concentration range exist.

We therefore decided to perform a systematic kinetic study on a suitable compound, which should be sufficiently stable to be isolated and characterized. The complex ion  $\text{NiL}_2^{3+}$  ( $L=1,4,7$ -triazacyclononane, tacn) was found to be the desired candidate. The existence of six amine nitrogen atoms in two distinct nine-membered rings affords octahedral coordination in a minimum of strain [25].

\*Lehrstuhl III, Institut für anorg. Chemie der Universität zu Köln (Professor Th. Kruck).

\*\*Author to whom correspondence should be addressed.

## Experimental

$\text{NiL}_2(\text{ClO}_4)_2$  and  $\text{NiL}_2(\text{ClO}_4)_3$  were prepared by literature methods [26]. *Anal. Calc.* for  $\text{NiL}_2(\text{ClO}_4)_2$ : C, 27.93; H, 5.86; N, 16.29; Ni, 11.38. *Found*: C, 27.7; H, 5.7; N, 16.1; Ni, 11.4%. *Calc.* for  $\text{NiL}_2(\text{ClO}_4)_3$ : C, 23.42; H, 4.91; N, 13.66; Ni, 9.54. *Found*: C, 23.4; H, 4.9; N, 13.6; Ni, 9.6%.

$\text{NiL}(\text{H}_2\text{O})_3\text{Cl}_2$ : 0.12 g (0.93 mmol) 1,4,7-triazacyclononane dissolved in 9 ml EtOH was added to a stirred solution of 0.22 g (0.90 mmol)  $\text{NiCl}_2\cdot 6\text{H}_2\text{O}$  in 18 ml EtOH. The blue product crystallized within 24 h. It was recrystallized from water, washed with EtOH and ether and dried in air; yield 0.10 g (36%). *Anal. Calc.* for  $\text{NiL}(\text{H}_2\text{O})_3\text{Cl}_2$ : C, 23.03; H, 6.77; N, 13.43; Ni, 18.76. *Found*: C, 22.4; H, 6.4; N, 13.1; Ni, 18.5%. All solutions were prepared from distilled deionized water and analytical pure reagents.

UV-Vis spectra were recorded on Cary 14 or 2300 instruments. Measurements of the slow kinetics (acid and neutral solutions) were performed on a Zeiss PMQ4 single beam photometer. The stopped-flow equipment used for the fast kinetic and spectroscopic measurements (alkaline solutions) was either an Optical Multichannel Synchron Analyser (OSMA, Spectroscopic Instruments), a DIONEX stopped-flow apparatus with a specially designed data transfer and processing system [27] or a SFA-11 Rapid Kinetics Accessory (HI-Tech Scientific Ltd) in combination with spectrometer and oscilloscope. For the pH measurements a digital pH

meter Knick 641 with a Schott N 61 glass electrode was used.

Cyclic voltammograms were recorded on a Methrom electrochemical system consisting of a polarecord model E506, a VA-scanner model E612, and a Rohde & Schwarz XY-recorder ZSK2. The working electrode was a stationary platinum microelectrode. The reference electrode was an Ag/AgCl electrode in saturated aqueous KCl. The experiments were performed under argon atmosphere and in argon saturated water containing 0.1 M sodium perchlorate at 22 °C.

The kinetic measurements were carried out at  $24 \pm 0.2$  °C in air saturated solutions. Preliminary experiments in the concentration range where the second order reaction dominates, had shown that the reaction rate was not affected by saturation with nitrogen. The general appearance of the UV-Vis spectra of  $\text{NiL}_2^{3+}$  did not alter during the reaction, neither in  $\text{HClO}_4$  nor in NaOH or in buffered solutions. Thus, the absorbance at any wavelength could be taken as a measure for the change in Ni(III) concentration with time.

## Results

### Spectroscopy

The spectroscopic data of  $\text{NiL}_2^{2+}$  and  $\text{NiL}_2^{3+}$  are compiled in Table 1. The data from the various references [14, 26, 28] agree in the positions of the maxima, but show large deviations in the absorptivity coefficients. We therefore felt it necessary to redetermine the absorption data, since exact values were necessary for the kinetic measurements. The results of the elementary analysis and repeated determinations on these complexes suggest that our results should be accepted within the stated error limits. Table 1 also includes the data of  $\text{NiL}(\text{H}_2\text{O})_3^{2+}$  and  $\text{Ni}_{\text{aq}}^{2+}$ , which are two possible decomposition products of  $\text{NiL}_2^{3+}$ . The Table further

shows that  $\text{NiL}_2^{3+}$  absorbs at 310 nm with  $\epsilon \approx 10^4 \text{ M}^{-1} \text{ cm}^{-1}$  whereas all Ni(II) species involved have absorptivity coefficients below 20, i.e. the reduction products do not interfere with the spectrophotometric determination of  $\text{NiL}_2^{3+}$ .

### Preliminary observations and stoichiometry of the reduction reaction

While the decomposition of  $\text{NiL}_2^{3+}$  in 1 mM  $\text{HClO}_4$  is very slow (half-life  $\approx 2$  weeks in a solution containing 0.05 mM  $\text{NiL}_2(\text{ClO}_4)_3$ ) it is considerably accelerated by increasing the pH. If concentrated NaOH is quickly added to such a slightly acid solution, an immediate color change from gold-brown to deep blue is observed. The blue color disappears within less than a second and is replaced by a faint pink, similar to the color of  $\text{NiL}_2^{2+}$ .

In a titration experiment 50 mg  $\text{NiL}_2(\text{ClO}_4)_3$  were dissolved in 2.5 ml 0.1 N NaOH. The resulting solution was titrated with 0.01 N  $\text{HClO}_4$  using methyl red as indicator. In comparison with a test solution containing  $\text{NiL}_2(\text{ClO}_4)_2$  and NaOH, the pH range of the indicator's color change was considerably broadened. 0.95 equivalents of  $\text{OH}^-$  were consumed per reacted nickel(III) ion. The buffer properties of the solution can be explained with released ligands or ligand fragments that act as weak bases during the titration.

Adding 9 M aqueous  $\text{NaClO}_4$  to a completely reacted solution yielded a pink precipitate which was identified as  $\text{NiL}_2(\text{ClO}_4)_2$  by IR spectroscopy. An identically treated test solution of  $\text{NiL}_2^{2+}$  allowed a correction for substance losses during the precipitation procedure. Exactly 50% of the reacted  $\text{NiL}_2^{3+}$  was transformed into  $\text{NiL}_2^{2+}$ . The remaining Ni(II) could not be precipitated by dimethylglyoxime; hence a strongly coordinating ligand was still attached to the Ni(II) ion. That means that only one ligand has been shedded from one of two reacting  $\text{NiL}_2^{3+}$  ions.

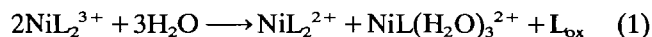
TABLE 1. UV-Vis data of  $\text{NiL}_2^{2+}$  and  $\text{NiL}_2^{3+}$  in aqueous solution

Compound	Solvent	$\lambda_{\text{max}}$ (nm) ( $\epsilon_{\text{max}}$ ( $\text{M}^{-1} \text{ cm}^{-1}$ ))	Reference
$\text{NiL}_2(\text{ClO}_4)_3$	0.1 N $\text{HClO}_4$	269 ( $9.54 \pm 0.05$ ) $\times 10^3$	310 ( $9.8 \pm 0.1$ ) $\times 10^3$ 562 ( $42.3 \pm 0.5$ )
			312 ( $7.2 \times 10^3$ ) 570 (65)
			312 ( $10.1 \pm 0.2$ ) $\times 10^3$
$\text{NiL}_2(\text{ClO}_4)_2$	$\text{H}_2\text{O}$	328 ( $5.05 \pm 0.05$ )	506.5 ( $5.5 \pm 0.1$ ) 802.5 ( $7.6 \pm 0.1$ ) 860sh
		308 (12)	505 (5) 800 (7) 870sh
		322 (11)	504 (11) 799 (16)
$\text{NiL}_2\text{Cl}_2$	$\text{H}_2\text{O}$	310 (12) 500 (9)	800 (9) 870 sh 28
$\text{NiL}_2(\text{NO}_3)_2$	$\text{H}_2\text{O}$	308 (16)	505 (5) 800 (7) 870sh 28
$\text{NiL}(\text{H}_2\text{O})_3\text{Cl}_2$	$\text{H}_2\text{O}$	356 ( $4.7 \pm 0.2$ )	579 ( $3.8 \pm 0.2$ ) 780(sh) 951 ( $13.0 \pm 0.2$ )
		334 (5)	575 (4) 877(sh) 961 (14) 28
$\text{Ni}(\text{H}_2\text{O})_6\text{Cl}_2$	$\text{H}_2\text{O}$	393 ( $5.4 \pm 0.2$ )	460(sh) 654 ( $2.0 \pm 0.2$ ) 720 ( $2.3 \pm 0.2$ ) 1175 (2.2) this work

\*Medium not stated.

Spectrophotometric evidence agrees with this result. The absorption of a 0.02 M aqueous solution that was left for three weeks in the dark at room temperature showed the superposition of the absorptions of  $\text{NiL}_2^{2+}$  and  $\text{NiL}(\text{H}_2\text{O})_3^{2+}$ . Figure 1 compares the 2nd derivative spectra of the reaction mixture with that of the presumed reaction products and Fig. 2 shows the spectrum of the reaction mixture and a simulated spectrum of a 1:1 mixture of  $\text{NiL}_2^{2+}$  and  $\text{NiL}(\text{H}_2\text{O})_3^{2+}$ .

The results obtained so far indicate the following stoichiometry for both alkaline and acid solutions (apart from the occurrence of acid base equilibria of the coordinated water molecules)



with  $\text{L}_{\text{ox}}$  a two-electron oxidation product of triaza-cyclonane. The overall reaction must therefore be a two-electron process.

In order to assess the role of  $\text{OH}^-$ , whether it acts as base or reductant, the reaction of  $\text{NiL}_2^{3+}$  with  $\text{Br}^-$  was studied. On account of their almost identical redox potentials ( $\text{OH}/\text{OH}^- + 1.89$ ,  $\text{Br}/\text{Br}^- + 1.93$  V) [29],  $\text{Br}^-$

should react as easily with  $\text{NiL}_2^{3+}$  as  $\text{OH}^-$ , if the hydroxide ion is oxidized by the nickel(III) ion. Adding a 170-fold excess of  $\text{NaBr}$  to a solution of  $\text{NiL}_2(\text{ClO}_4)_3$  caused only a small change in hue. The precipitate obtained by a subsequent addition of a 9 M  $\text{NaClO}_4$  solution was IR spectroscopically indistinguishable from pure  $\text{NiL}_2(\text{ClO}_4)_3$ . Thus a deprotonated complex with enhanced reactivity must be postulated as the primary reaction product. The identity of the observed blue intermediate with deprotonated  $\text{NiL}_2^{3+}$  can be confirmed from its immediate appearance in the stopped-flow experiments, where the strong increase of an absorption at 650 nm arose simultaneously with the mixing of  $\text{NiL}_2^{3+}$  and  $\text{OH}^-$  ( $\leq 5$  ms) in agreement with a diffusion controlled acid base reaction. The spectrum of the blue intermediate as obtained with the OSMA apparatus (mixing time  $\approx 30$  ms) is shown in Fig. 3. (Due to the limited spectral range of the apparatus the spectrum could only be recorded between 330 and 550 nm. Thus, the absorption maximum responsible for the blue color is not shown.)

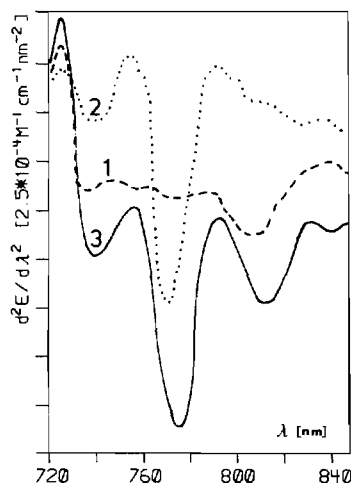


Fig. 1. 2nd derivative spectra of:  $\text{NiL}_2^{2+}$  (1);  $\text{NiL}(\text{H}_2\text{O})_3^{2+}$  (2); solution of  $\text{NiL}_2^{3+}$  in water after three weeks at room temperature (c. 22 °C) (3). For concentrations see Fig. 2.

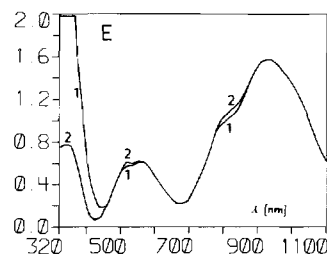


Fig. 2. Absorption spectrum of the reaction mixture corresponding to a 0.2 M solution (1) and superposition of the spectra of equimolar solutions of  $\text{NiL}_2^{2+}$  and  $\text{NiL}(\text{H}_2\text{O})_3^{2+}$ , calculated for 0.1 M solutions (2); actual solutions 0.02, 0.04 and 0.06 M, respectively.

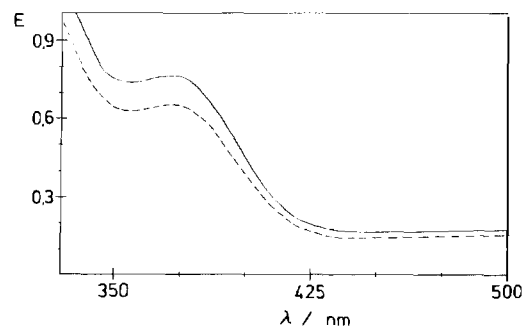


Fig. 3. Vis absorption spectra of  $3 \times 10^{-4}$  M  $\text{NiL}_2^{3+}$  in alkaline solution, extrapolated to zero time; ionic strength adjusted with  $\text{NaClO}_4$ ; solid line:  $c_{\text{OH}^-} = 5 \times 10^{-3}$  M, broken line:  $c_{\text{OH}^-} = 0.5$  M.

#### Cyclovoltammetry (CV)

Cyclovoltammograms were recorded from  $2 \times 10^{-3}$  and  $2 \times 10^{-4}$  M  $\text{NiL}_2(\text{ClO}_4)_2$  solutions at various pH values. Acid solutions gave quasireversible CV curves with anodic ( $E_{\text{pA}2}$ ) and cathodic ( $E_{\text{pC}2}$ ) peak potentials of 0.81 and 0.74 V versus  $\text{Ag}/\text{AgCl}$ , respectively, in agreement with previous determinations [12, 26]. On increasing the pH, the CV curves remained unchanged until pH 8 (Fig. 4(a)). Then an irreversible oxidation peak appeared at  $E_{\text{pA}1} = 0.6$  V that grew on further increasing the pH value\* (Fig. 4(b)–(d)). A new peak pair with  $E_{\text{pA}3} = 0.57$  and  $E_{\text{pC}3} = 0.54$  V appeared above pH 11. It replaced the three peaks mentioned above. We assign this pair to a two-electron step on account

\*We hesitate to assign this peak to the oxidation of a deprotonated  $\text{Ni}^{2+}$  species, because we did not observe any change in the absorption spectra of  $\text{NiL}_2^{2+}$  when hydroxide ion was added up to 1 M. A referee, however, pointed out, that “also minor components might have a major effect on the current”.

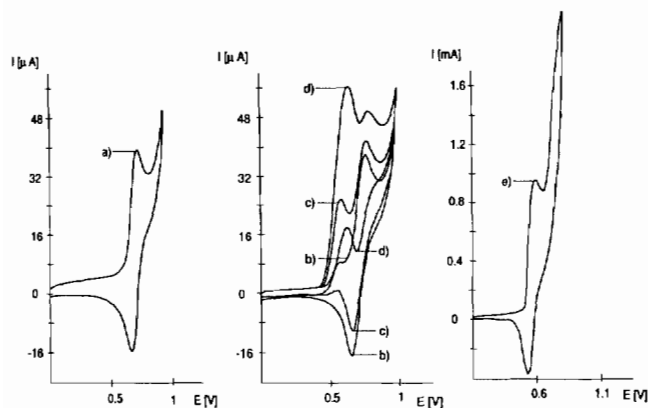


Fig. 4. Cyclovoltammograms of  $2 \times 10^{-3}$  M  $\text{NiL}_2(\text{ClO}_4)_2$  in 0.1 M  $\text{Na}(\text{OH}, \text{ClO}_4)$  vs.  $\text{Ag}/\text{AgCl}$ , scan rate  $30 \text{ mV s}^{-1}$ . (a) pH 7.5; (b) pH 9.9; (c) pH 10.5; (d) pH 11.0; (e) of  $2 \times 10^{-4}$  M  $\text{NiL}_2(\text{ClO}_4)_2$  in 0.1 M  $\text{Na}(\text{OH}, \text{ClO}_4)$  at pH 11.7 vs.  $\text{Ag}/\text{AgCl}$ , scan rate  $30 \text{ mV s}^{-1}$ .

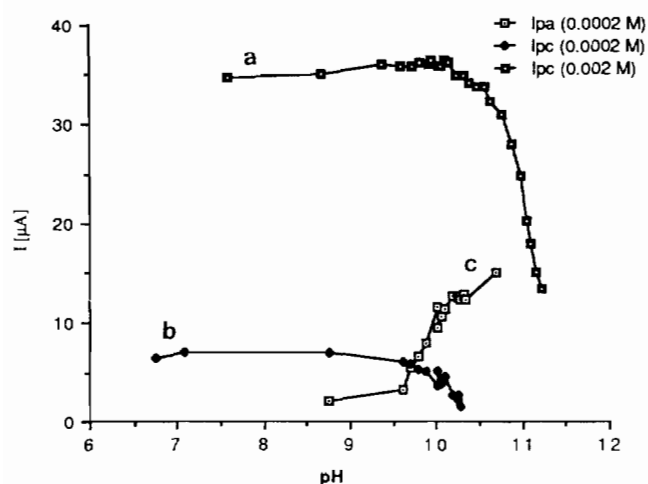


Fig. 5. pH dependence of the peak currents in the cyclovoltammograms of  $\text{NiL}_2(\text{ClO}_4)_2$  in 0.1 M  $\text{Na}(\text{OH}, \text{ClO}_4)$ ; potentials vs.  $\text{Ag}/\text{AgCl}$ , scan rate  $30 \text{ mV s}^{-1}$ . (a) and (b): Cathodic currents at 0.47 V. (a):  $2 \times 10^{-3}$  M, (b):  $2 \times 10^{-4}$  M, (c): anodic current at 0.64 V in  $2 \times 10^{-4}$  M solution.

of its peak potential difference and its peak currents (Fig. 4(e)). We found no indication of a reduction peak that could be assigned to the deprotonated species. The interpretation of the pH dependence is complicated, because the deprotonation and the  $\text{H}^+$  production in the course of the decomposition of the electrochemically generated  $\text{NiL}_2^{3+}$  decrease the pH at the electrode surface. Figure 5 shows the dependence of the cathodic peak current as a function of the pH value of the bulk solution. The sharp decrease in peak current above pH 10 in the  $10^{-4}$  M solution sets an upper limit to the  $\text{p}K_a$  value of  $\text{NiL}_2^{3+}$ , i.e.  $\text{p}K_a \leq 10$ .

#### Reaction order

The logarithmic form of the general equation for an  $n$ th order rate law reads

$$\ln(\text{dc}/\text{dt}) = n \ln c + \ln k_n \quad (2)$$

Values of  $\text{dc}/\text{dt}$  as a function of  $c$  were obtained by observing the decay of 0.6 to 2.0 mM solutions in 0.1/0.1 M acetate buffer (pH=4.66) over a period of  $c$ . 20 min. During this time only 5 to 10% of the complex had reacted and the change in absorbance was linear, yielding a reaction order of  $n=1.66$ . If the observed fractional order was due to simultaneous first and second order reactions, a plot of  $c^{-1} \text{dc}/\text{dt}$  versus  $c$  should be linear

$$-c^{-1} \text{dc}/\text{dt} = k_I + k_{II}c \quad (3)$$

as was the case. From slope and intercept we obtained  $k_I = 2.8 \times 10^{-5} \text{ s}^{-1}$  and  $k_{II} = 4.0 \times 10^{-2} \text{ M}^{-1} \text{ s}^{-1}$ .

#### pH dependence of the reaction rate

On account of the  $\text{OH}^-$  consumption during the reaction, reasonable kinetic data are obtainable only if  $c_{\text{H}^+}$  is held constant. Buffered solutions did not prove to be suitable, because the rates were found to depend on the buffer anions. For example, in phosphate and phthalate buffers of both pH 5.8 and ionic strength 0.14 M the first order rate constants were  $k_I = 16 \times 10^{-5}$  and  $6 \times 10^{-5} \text{ s}^{-1}$ , respectively. Consequently, large excesses of  $\text{H}^+$  and  $\text{OH}^-$  were applied.

At pH 3 the decomposition rate was sufficiently slow that initial slopes could be determined with reasonable accuracy. Figure 6 shows the concentration dependence according to eqn. (3). From slope and intercept  $k_I = (1.1 \pm 0.1) \times 10^{-6} \text{ s}^{-1}$  and  $k_{II} = (3.55 \pm 0.1) \times 10^{-3} \text{ M}^{-1} \text{ s}^{-1}$  were obtained.

Due to the rather low degrees of conversions ( $\leq 30\%$ ) both first and second order plots gave reasonably good linear fits (correlation  $> 0.99$ ). The apparent rate constants thus obtained were concentration dependent. However, extrapolation to  $c=0$  yielded  $k_I = (6.6 \pm 2.7) \times 10^{-7} \text{ s}^{-1}$  and extrapolation to  $c = \infty$  yielded  $k_{II} = (3.50 \pm 0.1) \times 10^{-3} \text{ M}^{-1} \text{ s}^{-1}$ . This method had the advantage that all data points could be included in the calculation.

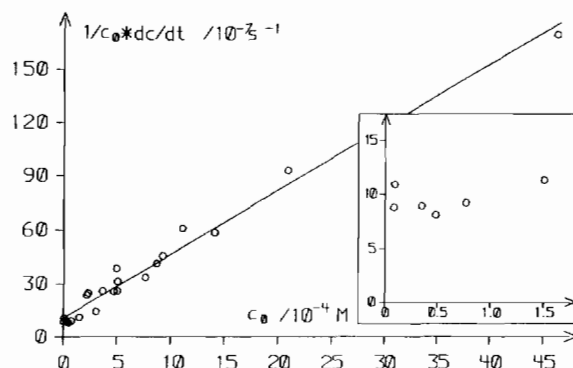


Fig. 6. Concentration dependence of the initial decomposition rate of  $\text{NiL}_2^{3+}$  in 0.1 M  $(\text{Na}, \text{H})\text{ClO}_4$ , pH=3.

Predominantly first order dependence is to be expected, if  $k_I \geq 5k_{II}c$  or  $c \leq 6 \times 10^{-5}$  M, according to the data obtained at pH 3 and in acetate buffer. For  $c \geq 5 \times 10^{-3}$  M the second order path is expected to dominate. Experimentally, first order plots yielded  $k_I = (7.6 \pm 0.6) \times 10^{-7} \text{ s}^{-1}$  (average of 5 runs) in the concentration range between  $10^{-5}$  and  $10^{-4}$  M. These values are in agreement with the methods where both reaction paths were considered.

Solutions containing initial concentrations of 0.06 mM for obtaining the first order path and of 10.8 mM for the second order path were studied at various acid concentrations. The rate data determined from the initial rates are summarized in Table 2.

The pH decrease in the course of the reaction was followed on some solutions prepared without addition of acid (natural pH  $6 \pm 0.2$ ). Figure 7 shows the change in hydrogen ion concentration for three different initial concentrations of  $\text{NiL}_2^{3+}$ . After an initial phase, where no hydrogen ion was produced, the hydrogen ion concentration increased linearly with decreasing Ni(III)

TABLE 2. Decomposition rates of  $\text{NiL}_2(\text{ClO}_4)_3$  in (H, Na)ClO<sub>4</sub> solution at 24 °C

$c_{\text{H}^+}$ (M)	Concentration of (H, Na)ClO <sub>4</sub> (M)	$k_I$ (s <sup>-1</sup> )	$k_{II}$ (M <sup>-1</sup> s <sup>-1</sup> )
		$c_{\text{Ni}} =$ $6 \times 10^{-5}$ M	$c_{\text{Ni}} =$ $1.08 \times 10^{-2}$ M
0.1	0.1		$0.93 \times 10^{-4}$
0.075	0.1		$1.05 \times 10^{-4}$
0.05	0.1		$1.28 \times 10^{-4}$
0.02	0.1		$2.35 \times 10^{-4}$
0.015	0.1		$2.86 \times 10^{-4}$
0.01	0.1		$4.05 \times 10^{-4}$
$2.5 \times 10^{-3}$	1	$2.2 \times 10^{-7}$	
$1 \times 10^{-3}$	1	$5.9 \times 10^{-7}$	
$1 \times 10^{-3}$	0.1	$1.1 \times 10^{-6a}$	$3.55 \times 10^{-3a}$
$2.5 \times 10^{-4}$	1	$2.1 \times 10^{-6}$	

<sup>a</sup>Mixed order analysis according to eqn. (3),  $10^{-5} \leq c_{\text{Ni}} \leq 5 \times 10^{-3}$ .

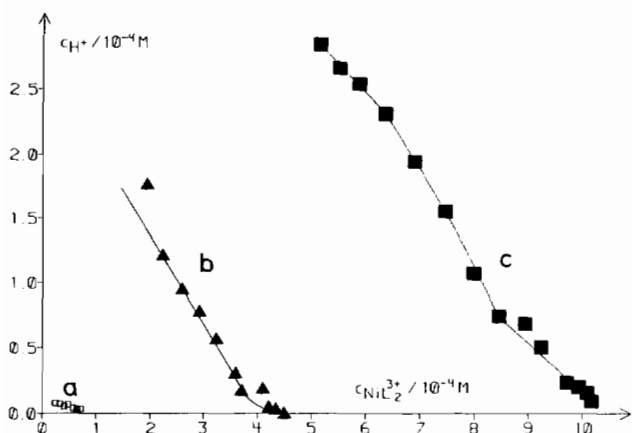


Fig. 7. Change in hydrogen concentration during decomposition  $\text{NiL}_2^{3+}$  in 0.1 M NaClO<sub>4</sub>.

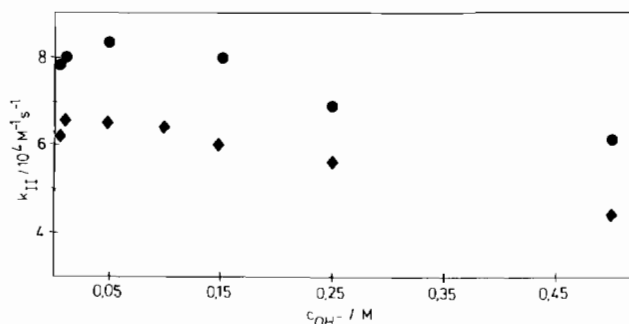


Fig. 8. Second order rate constants for the decomposition of  $\text{NiL}_2^{3+}$  in alkaline solution (1 M Na(OH<sup>-</sup>; ClO<sub>4</sub><sup>-</sup>) at 24 °C; observation at 375 (●) and 650 (◆) nm.

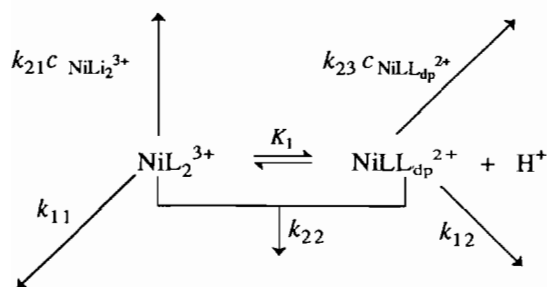
concentration. The slope approached a value of 1 for concentrations where only the second order process was effective.

In alkaline solution the decomposition reaction was so fast that the stopped-flow technique had to be applied. As in buffered solutions first and second order reactions were observed, depending on the complex concentrations. However, the corresponding ranges were shifted to lower concentrations by two orders of magnitude, compared with those in acetate buffer. Strictly first and second order behavior occurred at  $c_{\text{NiL}_2^{3+}} < 0.001$  and  $> 0.1$  mM, respectively. Due to the small concentrations required, first order rate measurements were accompanied by large experimental errors. Therefore, no OH<sup>-</sup> dependence of  $k_I$  was recorded. Only a selected concentration of  $c_{\text{OH}^-} = 50$  mM ( $k_I = 0.5 \pm 0.3 \text{ s}^{-1}$ ) was studied. Figure 8 shows the hydroxide ion dependence of  $k_{II}$  observed at 375 and 650 nm. The different results at those wavelengths are probably caused by errors in the determinations of the absorptivity coefficients of the deprotonated species.  $\epsilon_{375} = 1250 \text{ M}^{-1} \text{ cm}^{-1}$  was determined by extrapolation to  $t=0$ , using the data obtained on the DIONEX apparatus. This value is probably somewhat too large because the mixing time was included in the extrapolation.  $\epsilon_{650} = 730 \text{ M}^{-1} \text{ cm}^{-1}$ , on the other hand, was obtained from data measured with the SFA-11 stopped-flow equipment immediately after mixing. This value is probably too small because the reaction that occurred during mixing was neglected.

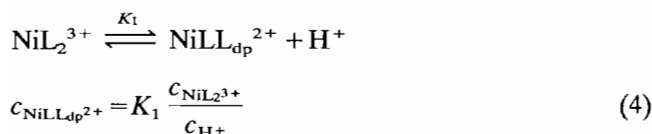
## Discussion

The results obtained shall be discussed on the basis of reaction Scheme 1 with  $\text{NiLL}_{\text{dp}}^{2+}$  the N-deprotonated complex.

The acid-base equilibrium is assumed to be fast compared with the subsequent decomposition reactions.



Scheme 1.



The overall conversion has to be balanced

$$dc_{\text{NiL}_2^{3+}}/dt + dc_{\text{NiLL}_{\text{dp}}^{2+}}/dt + dc_{P_1}/dt + dc_{P_{II}}/dt = 0 \quad (5)$$

with  $P_1$  and  $P_{II}$  denoting the sum of all products of first and second order reactions, respectively. If only the monomolecular decomposition takes place, the basic kinetic equation reads

$$-dc_{\text{NiL}_2^{3+}}/dt - dc_{\text{NiLL}_{\text{dp}}^{2+}}/dt = dc_{P_1}/dt$$

$$= k_{11}c_{\text{NiL}_2^{3+}} + k_{12}c_{\text{NiLL}_{\text{dp}}^{2+}} \quad (6)$$

As the UV-Vis spectrum of  $\text{NiL}_2^{3+}$  in  $\text{HClO}_4$  is not sensitive to  $c_{\text{H}^+}$ , only  $\text{NiL}_2^{3+}$  was observed under acid conditions. Elimination of  $c_{\text{NiLL}_{\text{dp}}^{2+}}$  by use of eqn. (4) yields

$$-dc_{\text{NiL}_2^{3+}}/dt = \frac{k_{11}c_{\text{H}^+} + k_{12}K_1}{K_1 + c_{\text{H}^+}} c_{\text{NiL}_2^{3+}} \quad (7)$$

The analogous treatment of the bimolecular reaction gives

$$-dc_{\text{NiL}_2^{3+}}/dt$$

$$= \frac{k_{21}c_{\text{H}^+} + k_{22}K_1 + k_{23}K_1^2c_{\text{H}^+}^{-1}}{K_1 + c_{\text{H}^+}} c_{\text{NiL}_2^{3+}}^2 \quad (8)$$

Assuming  $c_{\text{H}^+} \gg K_1$  the following simplified equations for  $k_1$  and  $k_{II}$  are obtained from eqns. (7) and (8):

$$k_1 = k_{11} + k_{12}K_1c_{\text{H}^+}^{-1} \quad (9)$$

$$k_{II} = k_{21} = k_{22}K_1c_{\text{H}^+}^{-1} \quad (10)$$

With this,  $k_{11} < 10^{-8} \text{ s}^{-1}$  ( $I = 1 \text{ M}$ ),  $k_{12}K_1 = (5.26 \pm 0.2) \times 10^{-10} \text{ M s}^{-1}$  ( $I = 1 \text{ M}$ ),  $k_{21} = (6.0 \pm 0.6) \times 10^{-5} \text{ M}^{-1} \text{ s}^{-1}$  ( $I = 0.1 \text{ M}$ ), and  $k_{22}K_1 = (3.43 \pm 0.2) \times 10^{-6} \text{ s}^{-1}$  ( $I = 0.1$ ) are obtained from the data of Table 2.

The disappearance of the deprotonated species was observed in alkaline solution. The rate law for the first order reaction is identical to that in acid solution,

because

$$\frac{1}{c_{\text{NiL}_2^{3+}}} \frac{dc_{\text{NiL}_2^{3+}}}{dt} = \frac{1}{c_{\text{NiLL}_{\text{dp}}^{2+}}} \frac{dc_{\text{NiLL}_{\text{dp}}^{2+}}}{dt} \quad (11)$$

on account of the equilibrium (eqn. (4)). The second order rate constant, however, is different

$$k'_{II} = \frac{k_{22}c_{\text{H}^+} + k_{23}K_1 + \frac{k_{21}}{K_1}c_{\text{H}^+}^2}{K_1 + c_{\text{H}^+}} \quad (12)$$

where the quadratic term in eqn. (12) may be neglected at higher pH values

$$k'_{II} = \frac{k_{22}K_w + k_{23}K_1c_{\text{OH}^-}}{K_1c_{\text{OH}^-} + K_w} \quad (13)$$

with  $K_w = c_{\text{OH}^-}c_{\text{H}^+}$ .

Figure 8 shows that  $k'_{II}$  reaches a plateau for  $0.01 \text{ M} \leq c_{\text{OH}^-} \leq 0.1 \text{ M}$ , where it is rather insensitive to  $c_{\text{OH}^-}$ . The stopped-flow experiments further showed that the initial concentrations of the deprotonated species were independent of pH from  $10^{-3} \text{ M}$  NaOH onwards. This implies that  $\text{NiL}_2^{3+}$  is nearly entirely deprotonated under these conditions, i.e.  $K_1 \gg c_{\text{H}^+}$ . Then from eqns. (7) and (12) it follows that  $k_1 = k_{12}$  and  $k'_{II} = k_{23}$ . Averaging  $k_1$  and  $k'_{II}$  in the plateau region yielded  $k_{12} = 0.5 \pm 3 \text{ s}^{-1}$  ( $I = 1 \text{ M}$ ) and  $k_{23} = (7.3 \pm 0.8) \times 10^4 \text{ M}^{-1} \text{ s}^{-1}$  ( $I = 1 \text{ M}$ ).

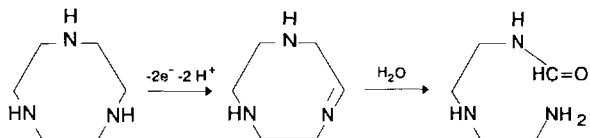
Estimating  $K_1$  from the first order rates in alkaline and acid solution yields  $\text{p}K_1 \approx 9$ . This order of magnitude is in reasonable agreement with the electrochemical estimation, although large errors may be involved in the first order rates. Assuming  $K_1 = 10^{-9} \text{ M}$  yields  $k_{22} = 3 \times 10^3 \text{ M}^{-1} \text{ s}^{-1}$ .

Above  $0.1 \text{ M}$  NaOH the second order rate constant decreased with increasing hydroxide concentration (Fig. 8). In this region the second deprotonation step of  $\text{NiL}_2^{3+}$  might be effective. On the other hand, this is also the pH region where the two-electron oxidation peak  $E_{\text{pA}_3}$  occurred in the CV experiments, which was the least positive peak observed. Its corresponding oxidation product should be more stable against reduction than the other species. Since there were no indications in the transient spectra on other intermediates besides  $\text{NiLL}_{\text{dp}}^{2+}$ , no further conclusions can be drawn.

The apparent first order rate may be strongly affected by the interference of impurities, as for instance by dissolved oxygen. The initial phase in the  $\Delta c_{\text{H}^+}$  versus  $c_{\text{Ni}}$  plots (Fig. 7), where no hydrogen ion was produced, was obviously caused by some reaction with impurities. This reaction dominated at the very low concentrations that were necessary for observing the first order decay. On account of those difficulties we shall only discuss the mechanism of the second order process.

The stoichiometry of the overall reaction eqn. (1) implies a two-electron redox process that is initiated by the deprotonation of  $\text{NiL}_2^{3+}$ . The deprotonated species reacts with another nickel complex in an outer sphere redox process.

In analogy to the oxidation of tertiary amines by  $\text{Fe}(\text{CN})_6^{3-}$  [30], the tetraaza-macrocyclic complexes of Ni(III) [18, 19, 24, 31, 32] and the amine complexes of Cu(III) [33], Fe(III) [34–37] and Ru(III) [38, 39] we propose the following mechanism.



This mechanism accounts for the production of one proton for one electron transferred to Ni(III). The open chained amine is presumably a weaker ligand and will easily dissociate from Ni(II).

The deprotonated nickel complex reacts in a similar manner to the corresponding iron complex [37]. It is more reactive, however, in accordance with the more positive reduction potential of Ni(III). Spectroscopic data and acidity constants of deprotonated Ni(III) complexes are known only for some unsaturated tetraaza macrocycles [31, 32]. Both show some resemblance to those reported here for  $\text{NiL}_2^{3+}$ .

## Acknowledgements

We thank Professor van Eldik (Witten) and Professor Ilgenfritz (Köln) for permission to use and help with their kinetic equipment, and Professor Th. Kruck for his support with the electrochemical measurements. Financial assistance by the Verband der Chemischen Industrie is gratefully acknowledged.

## References

- J. Lati and D. Meyerstein, *Inorg. Chem.*, **11** (1972) 2393 and 2397.
- A. McAuley and C. Xu, *Inorg. Chem.*, **27** (1988) 1204.
- K. Kumar, F. P. Rotzinger and J. F. Endicott, *J. Am. Chem. Soc.*, **105** (1983) 7064.
- A. McAuley, O. Olubuyide, L. Spencer and P. R. West, *Inorg. Chem.*, **23** (1984) 2594.
- A. McAuley, P. R. Norman and O. Olubuyide, *J. Chem. Soc., Dalton Trans.*, (1984) 1501.
- A. McAuley and P. R. Norman, *Isr. J. Chem.*, **25** (1985) 106.
- A. McAuley, L. Spencer and P. R. West, *Can. J. Chem.*, **63** (1985) 1198.
- M. G. Fairbank, A. McAuley, P. R. Norman and O. Olubuyide, *Can. J. Chem.*, **63** (1985) 2983.
- M. G. Fairbank and A. McAuley, *Inorg. Chem.*, **26** (1987) 2844.
- E. Zeigerson, G. Ginzburg, N. Schwartz, Z. Luz and D. Meyerstein, *J. Chem. Soc., Chem. Commun.*, (1979) 241.
- E. Kimura, T. Koike, M. Yamaoka and M. Kodama, *J. Chem. Soc., Chem. Commun.*, (1985) 1341.
- L. Fabbrizzi, A. Perotti, A. Profumo and T. Soldi, *Inorg. Chem.*, **25** (1986) 4256.
- F. V. Lovecchio, E. S. Gore and D. H. Busch, *J. Am. Chem. Soc.*, **96** (1974) 3109.
- A. McAuley, P. R. Norman and O. Olubuyide, *Inorg. Chem.*, **23** (1984) 1938.
- H. Cohen, L. J. Kirschenbaum, E. Zeigerson, M. Jaacobi, E. Fuchs, G. Ginzburg and D. Meyerstein, *Inorg. Chem.*, **18** (1979) 2763.
- R. I. Haines and A. McAuley, *Inorg. Chem.*, **19** (1980) 719.
- M. G. Fairbank and A. McAuley, *Inorg. Chem.*, **25** (1986) 1233.
- R. I. Haines and A. McAuley, *Coord. Chem. Rev.*, **39** (1981) 77.
- E. K. Barefield and M. T. Mocella, *J. Am. Chem. Soc.*, **97** (1975) 4238.
- E. Zeigerson, G. Ginzburg, D. Meyerstein and L. J. Kirschenbaum, *J. Chem. Soc., Dalton Trans.*, (1980) 1243.
- E. Zeigerson, I. Bar, J. Bernstein, L. J. Kirschenbaum and D. Meyerstein, *Inorg. Chem.*, **21** (1982) 73.
- P. Morliere and L. K. Patterson, *Inorg. Chem.*, **21** (1982) 1833 and 1837.
- D. E. Linn, Jr., M. J. Dragan and D. E. Miller, *Inorg. Chem.*, **29** (1990) 4356.
- M. Jaacobi, D. Meyerstein and J. Lilie, *Inorg. Chem.*, **18** (1979) 429.
- A. Buttafava, L. Fabbrizzi, A. Perotti, A. Poggi, G. Poli and B. Seghi, *Inorg. Chem.*, **25** (1986) 1456.
- K. Wiegardt, W. Schmidt, W. Herrmann and H.-J. Küppers, *Inorg. Chem.*, **22** (1983) 2953.
- J. Kraft, S. Wieland, U. Kraft and R. van Eldik, *GIT Fachz. Lab.*, **31** (1987) 560.
- R. Yang and L. J. Zompa, *Inorg. Chem.*, **15** (1976) 1499.
- H. A. Schwarz and R. W. Dodson, *J. Phys. Chem.*, **88** (1984) 3643.
- D. H. Rosenblatt and E. P. Burrows, in S. Patai (ed.), *The Chemistry of Amino, Nitroso, and Nitro Compounds*, Interscience, London, 1982, p. 1085.
- H. Cohen, M. Nutkovich, D. Meyerstein and A. Shusterman, *Inorg. Chem.*, **23** (1984) 2361.
- A. Ulman, H. Cohen and D. Meyerstein, *Inorg. Chim. Acta*, **64** (1982) L127.
- T. A. Neubecker, S. T. Kirksey, Jr., K. L. Chellappa and D. W. Margerum, *Inorg. Chem.*, **18** (1979) 444.
- M. Goto, M. Takeshita, N. Kanda, T. Sakai and V. L. Goedken, *Inorg. Chem.*, **24** (1985) 582.
- H. E. Toma, A. M. C. Ferreira and N. Y. M. Iha, *Nouv. J. Chim.*, **9** (1985) 473.
- A. M. C. Ferreira and H. E. Toma, *J. Chem. Soc., Dalton Trans.*, (1983) 2051.
- K. Pohl, K. Wiegardt, W. Kaim and S. Steenken, *Inorg. Chem.*, **27** (1988) 440.
- S. E. Diamond, G. M. Tom and H. Taube, *J. Am. Chem. Soc.*, **97** (1975) 2661.
- M. J. Ridd and F. R. Keene, *J. Am. Chem. Soc.*, **103** (1981) 5733.